DEVELOPMENT OF THE DLR TAU-CODE FOR AEROSPACE APPLICATIONS

Dieter Schwamborn[1], Anthony D. Gardner[2], Heiko von Geyr[3], Andreas Krumbein[4], Heinrich Lüdeke[5], Arne Stürmer[6]

[1] DLR, Institute for Aerodynamics and Flow Technology, Göttingen, Germany, Dieter.Schwamborn@dlr.de
[2] DLR, Institute for Aerodynamics and Flow Technology, Göttingen, Germany, Tony.Gardner@dlr.de
[3] DLR, Institute for Aerodynamics and Flow Technology, Braunschweig, Germany, Heiko.vGeyr@dlr.de
[4] DLR, Institute for Aerodynamics and Flow Technology, Göttingen, Germany, Andreas.Krumbein@dlr.de
[5]DLR, Institute for Aerodynamics and Flow Technology, Braunschweig, Germany, Heinrich.Luedeke@dlr.de
[6] DLR, Institute for Aerodynamics and Flow Technology, Braunschweig, Germany, Arne.Stuermer@dlr.de

ABSTRACT *This paper gives an overview of the TAU-Code, DLR's system for complex flow simulations on unstructured hybrid grids. Starting from a short description of the system and its components, its basic capabilities are discussed. The remainder of the paper discusses a number of applications of varying complexity, such as transition prediction, influence of engine installation on high devices devices on a full aircraft configuration, flow about a generic Arianne-type launcher with fluid-structure interaction on the rocket nozzle or full aircraft simulations of a turbo-prop airplane or a complete delta wing configuration.*

1. INTRODUCTION

Computational Fluid Dynamics (CFD) has reached wide acceptance as a mature tool complementary to wind tunnel and flight tests. With increased reliability and quality it has found entrance into the engineering offices of the European aircraft industry. Accordingly, future aircraft development will more heavily rely on (multi-disciplinary) simulation in the design phase, as recently announced by Airbus in its motto: "More Simulation, Less Testing". For the future Airbus simulation environment, currently being built up, it has been decided to employ the DLR TAU-Code [9] as the CFD-tool for complex configurations simulated with hybrid unstructured grids. At the same time, the numerical methods have still to be improved to meet the constantly rising requirements with respect to accuracy and efficiency and to reduce the response time for complex simulations, even if the relevant geometries and underlying physical flow models become increasingly complex. While it was sufficient in many cases in the past to obtain correct tendencies and deltas for different modifications of a geometry the major challenge for CFD is now to deliver highly accurate results and correct trends for new configurations in order to become a reliable design tool in the process chains of the aeronautical industry.

This paper gives an overview on the TAU-Code, its current features and recent applications ranging from basic research over standard applications to complex configurations in aeronautics and aerospace.

2. THE DLR TAU-CODE

The DLR TAU code is actually not one code but a modern software system for the prediction of viscous and inviscid flows about complex geometries from the low subsonic to the hypersonic flow regime, employing hybrid unstructured grids composed of tetrahedrons, pyramids, prisms and hexahedrons. The system, in the following just called TAU, is composed of a number of modules and libraries to allow easier development, maintenance and reuse of the code or parts of it. The main modules of TAU can both be used as stand-alone tools with corresponding file I/O or within a Python scripting framework allowing for inter-module communication without file-I/O.

While TAU is mainly used for complex aircraft-type configurations (including coupling to structural and flight mechanics codes) there exist also extensions allowing the simulation of re-entry flows, i.e. real gas effects of oxygen and nitrogen or carbon dioxide can be taken into account. In order to allow efficient simulation of complex configurations with several ten million grid points TAU has been completely parallelized based on domain decomposition and the message passing concept using MPI.

The main modules of TAU:

- The pre-processing is used to prepare the metric of the grid. This metric is given by the volumes of the dual cells, normal vectors representing size and orientation of the faces of these cells and the geometric coordinates of the grid nodes. The connectivity of the grid is constructed by linking the two nodes on both sides of each face to the corresponding edge from the primary grid elements. This edge based data structure makes the solver independent of the element types in the primary grid and

enables the use of a multi-grid technique based on the agglomeration approach, which obtains coarse grids by fusing fine grid volumes.

- The solver is based on the compressible Navier-Stokes equations, employing Low Mach number pre-conditioning to extend its use into the incompressible flow regime. The spatial discretisation is second-order accurate both for the viscous and inviscid terms, where the latter are computed based on central or a variety of upwind schemes. Steady solutions are obtained via time integration based either on explicit Runge-Kutta schemes or an implicit LU-SGS scheme, both with additional convergence acceleration by multi-grid. For time accurate computations the dual time stepping approach of Jameson is employed. As the solver respects the geometric conservation law both grid deformation and bodies in arbitrary motion can be simulated.
- The grid adaptation, which is used to efficiently resolve detailed flow features in hybrid meshes, is based on local grid refinement and wall-normal mesh movement in semi-structured near-wall layers. The algorithm used allows also for de-refinement of earlier refined elements thus enabling the code to be used for unsteady time-accurate adaptation in unsteady flows.

Furthermore modules are available, which allow

- parallel partitioning of large computational grids in a requested number of domains at the start of simulation
- grid deformation to account for moderate changes of the geometry resulting from structural response on aerodynamic loads in coupled simulations or from an optimization technique during shape design. Here a very fast yet robust algebraic method has been developed based on an advancing front technique, allowing for e.g. wing tip deflections of one or several chord length.
- use of CHIMERA techniques, an important feature to efficiently simulate complex manoeuvring aircraft with moving control surfaces or handling of multi-body configurations. The current implementation of the Chimera technique can handle both steady and unsteady simulations with multiple moving bodies.

More recent developments, which are partly still in progress, include the use of structured algorithms in regions of structured hexahedral grids to increase performance and accuracy in these areas and the integration of a discrete adjoint solver used for aerodynamic shape optimization in viscous turbulent flows.

Turbulence and Transition modelling

The turbulence models implemented within the TAU code include linear and non-linear eddy viscosity models (EVM) spanning from one- and two-equation EVM through Reynolds-stress models to hybrid RANS-LES models. The standard turbulence model used is the Spalart-Allmaras model yielding highly satisfactory results for a wide range of applications while being numerically robust. The two equation models are k-ω based, with the Menter SST model being most popular. Recently, model specific "universal" wall-functions have been introduced to achieve a higher efficiency of the solver, especially for use in design or optimisation as well as for complex configurations where meshes with appropriate resolution in all wall areas are difficult to guarantee. The new formulations seem to deliver nearly as good results as the low Reynolds approach over a wide range of y+ values (for the first cell off the wall), while saving up to 75 % of computation time and 40 % of memory. Finally, there are options to perform Detached Eddy Simulations (DES) or Extra-Large Eddy Simulation (XLES).

Transition prediction is a relatively new module in TAU code, which comprises a number of different transition prediction approaches and can be applied to different types of configurations. Besides two e^N-database methods for Tollmien-Schlichting and cross flow instabilities, a fully automated linear stability code is available. The parameters of the laminar boundary layers which are determined along inviscid streamlines are either computed by a laminar boundary-layer code for swept tapered wings based on approximations for external conical flows or they are directly evaluated inside the TAU code using the solution from the RANS grid. Thus, the coupled system can be applied to complex configurations in an industrial context making use of the short computation times of the boundary-layer code, but allows alternatively to compute the necessary boundary-layer parameters from the RANS solution (provided a fine enough grid is available), e.g. when transition inside a laminar separation bubble has to be detected. Automatic transition prediction can be applied to 2D and 3D multi-element configurations of industrial relevance as shown in the first application of section 3.

3. APPLICATIONS

Automatic transition prediction

Figure 1 depicts results for a two-dimensional two-element airfoil configuration from [14] consisting of a main airfoil (based on the supercritical NLR 7301 airfoil) with a single-slotted trailing edge flap.

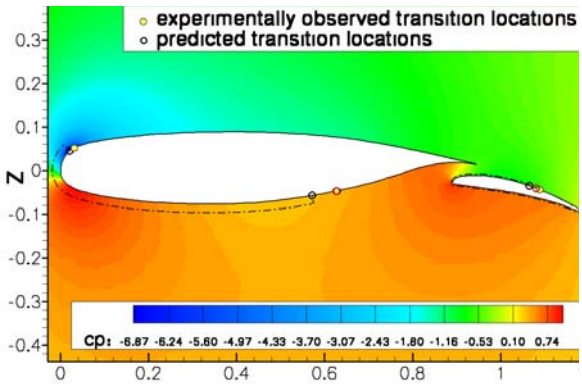

Fig. 1 Transition locations (circles), laminar regions (dashed line) and c_p-distribution

The computations were carried out for Reynolds number a $Re_\infty = 1.35\times10^6$ based on the main-airfoil chord, a Mach number $M_\infty = 0.185$ and an angle of attack (AoA) $\alpha = 6.0°$. In the figure, the experimentally observed (yellow) as well as the predicted transition locations are shown based on two different approaches. The first uses direct determination of the transition points using the N-factor curves from the linear stability code. These transition points are depicted as black hollow circles together with the corresponding laminar regions and the c_p-field showing good agreement with the experimental values.

The second approach applies an extrapolation technique for the N-factor envelope and can improve the results significantly which is the case for the lower surface of the main airfoil and the flap upper side as seen comparing the red hollow circles with the experimental ones. The accuracy of all predicted transition points is excellent. Figure 2 shows the transition lines and the laminar regions which were predicted for the DLR F11 model [6, 7] representing a modern transport aircraft with a three-element high-lift system consisting of a main wing with full span slat and flap. The results for Reynolds number $Re_\infty = 1.35\times10^6$, Mach number $M_\infty = 0.174$ and AoA $\alpha = 14°$ clearly show that it is not reliable to assume that transition lines are at constant chord-wise position over most of the wing as often used in RANS computations. In the inset in Figure 2 the predicted transition locations are compared to experimental ones determined during the EU-project EUROLIFT using two hot films on the slat and the main wing at about 68% half-span (solid blue line). Computed transition points at a nearby position (dashed line) reproduce the experimental position with very good accuracy.

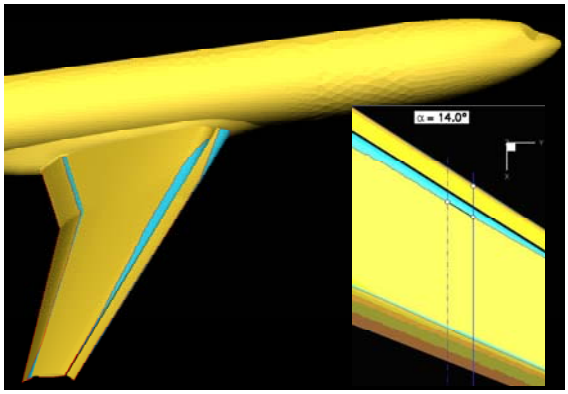

Fig. 2 High-lift configuration with transition lines and laminar regions (blue) on all three wing elements. Inset: Comparison with experiment.

Supporting experimentalists with the prediction of wind tunnel wall effects

Knowing effects of the wind tunnel on an experiment can help in selecting test points, in designing the experimental set-up and in evaluating test data. The DLR project iGREEN (Integrated Green Aircraft; 2007-2010) investigates the effects of increased aircraft elasticity due to new aerodynamic configurations or optimised structures. One work package concerns the wing-tailplane interference through buffet processes and includes experiments in the Transonic Wind tunnel Göttingen (TWG) in 2010. Here (Figure 3), a NLR7301 airfoil is to be attached to a flutter rig providing high-frequency pitching oscillations upstream of an elastic swept wing, as described in [3]. The resulting unsteady flow is used to excite a swept elastic wing mounted downstream in the tunnel, which has previously been used in the Aerostabil project [2]. In support of the experiment, RANS computations with TAU were started in 2007 to quantify the effects of the TWG side-wall boundary layer on the experiment, and to

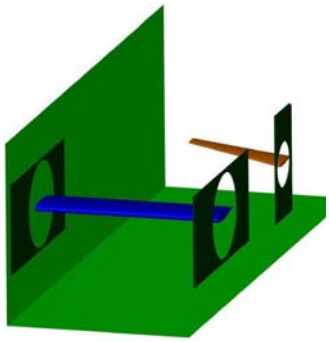

Fig. 3 Experimental setup

identify potential problems. Computations for the NLR7301 comparing results for viscous and inviscid wind-tunnel sidewalls identified significant changes due to the side-wall boundary layer at high Mach number and angle of attack (Figure 4). Here 3D separation areas forming in the corner of the wing-sidewall intersection act as displacing bodies which accelerate the flow, giving an effect vaguely similar to a reduced AoA. Further investigation using 2D computations with a corrected α could only approximately reproduce the effect shown due to the three-dimensionality of the flow.

As the elastic wing is fixed directly to the wind-tunnel sidewall the root of the wing is located within the wall boundary layer. Thus the decision where to place the instrumentation in the wing depends on the extent of the effects of the boundary layer on the wing. A comparison of the differences in pressure induced by the boundary layer on the side-wall (Figure 5) showed that positions with distance from the wall greater than 400 mm are best suited for instrumentation and thus helped considerably in preparing a successful validation experiment.

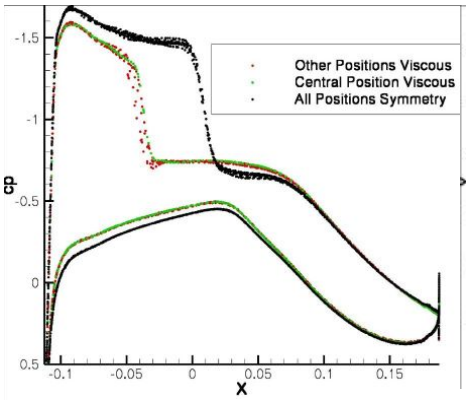

Fig. 4 Computed c_p distribution for viscous and inviscid tunnel walls

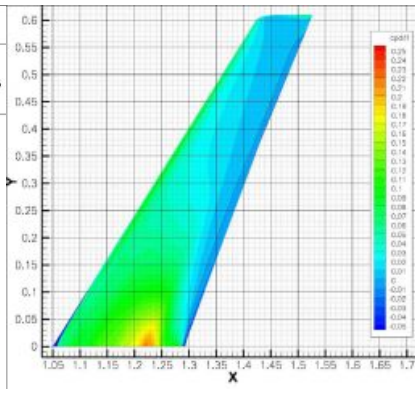

Fig. 5 Δc_p resulting from viscous and inviscid tunnel walls

Simulation of High-Lift Systems

The three-element high-lift system of commercial transport aircraft is well established and the interaction mechanisms between the three elements are in principle understood [10]. However, the geometry of realistic high-lift systems is more complicated and the interaction mechanisms are disturbed by vortical flows produced, e.g. by interaction with the flow about the engine nacelle. In the European project EUROLIFT II [8] the influence of a nacelle strake on the flow over the high-lift system was examined, leading to lift recovery which has evidently been demonstrated in wind tunnel tests.

A comparison of wind tunnel (W/T)) measurements from the LSWT (Airbus Bremen) and the numerical simulation [5] is shown in Figure 6, where it has to be noted that the experiment was conducted with closed wind tunnel walls and hence a certain influence of the tunnel walls on the measurements is expected. To clarify the reason of this off-set between the measured and computed lift curves, FOI as partner of EUROLIFT II performed CFD-computations for the case of the model without engine nacelle (so-called stage 1 configuration) installed in the ETW. In comparison with the computational results of the free-flight conditions (half model computation with symmetry condition) the wind tunnel wall influence was analyzed in [4]. Here it could be shown that the obtained off-set is at least partly due to the wall influence.

Computed and measured lift polars are cross plotted for three configurations: stage 1 without a nacelle, stage 2 with a nacelle and stage 3 with a strake on the nacelle. The dashed lines denote the measurements and the solid lines are assigned to the numerical results. While the correlation between lift and AoA seems to be shifted to higher alpha in the linear range of the lift curve, maximum lift is predicted within an accuracy of 1.5% for all three configurations. The highest lift (and lowest drag) is measured for the stage 1 configuration as also predicted by CFD. With the engine installation a significant loss of maximum lift (and an increase in drag) is measured. This influence of the engine installation on the global coefficients is captured by the numerical results. As the nacelle strake is added,

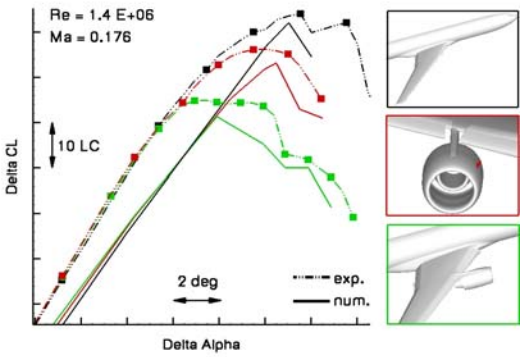

Fig. 6 Experimental vs. numerical lift

approximately 60 to 70% of the loss in maximum lift is recovered, which is again very well predicted by CFD. Adding the strake is not producing any noticeable drag increase according to the measurement which is consistently predicted by CFD (not shown).

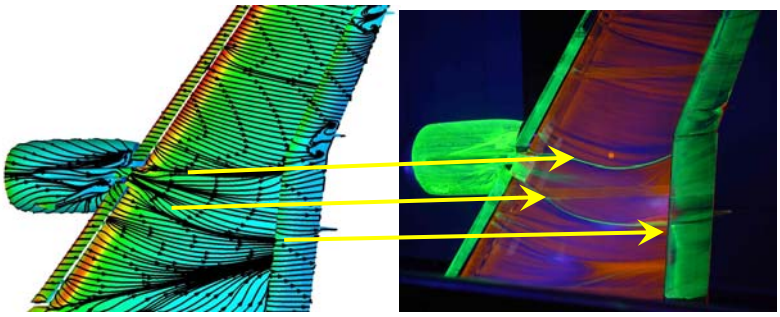

Fig. 7 Limiting streamlines at α=18.5°, Stage 3.

Figure 7 depicts the computed skin friction lines for the configuration with the strake in comparison to flow visualization from the wind tunnel test in the LSWT. All main flow features and effects as visible through the skin friction lines are captured by CFD. From this result and the discussed lift behavior it can be concluded that CFD is well capable to predict the strake effect within good accuracy.

The effect of the strake is indicated in Figure 8 showing a close up of the skin friction lines on the inner slat and the nacelle between nacelles without and with strake. The contour plots denote the c_{fx}-distribution on each configuration, where the red colour indicates negative c_{fx}-values and thus flow separation. The slat separation is clearly seen for the strake-less configuration. These results were obtained simulating the complete flow about the wing body configuration, including not only the engine nacelle but also the flap-track fairing of the complete lifting system as simulated in the wind tunnel.

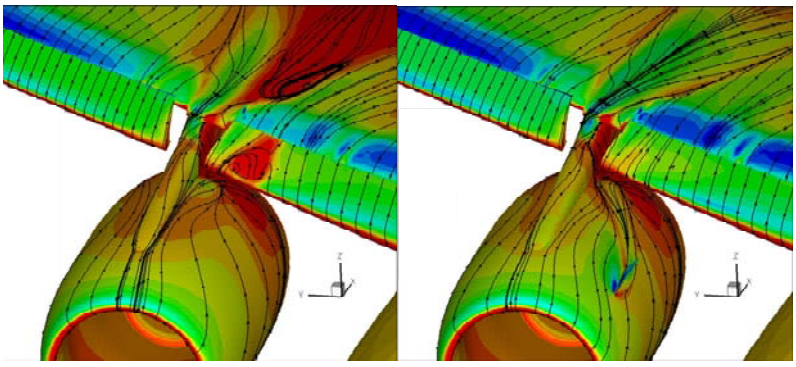

Fig. 8 Effect of nacelle strake on flow topology for Re=25·106 and α=17.5° (Stage 2 left; Stage 3 right picture).

Simulation of Propeller-Airframe Interaction Effects

Due to the flexibility resulting from the implementation of the Chimera technique as well as the availability of a comprehensive set of motion libraries the DLR TAU-Code is able to simulate the complex aerodynamic interactions between wing mounted propellers and the airframe. This type of simulation capability has been developed and validated in a number of studies [13]. One recent example is the simulation of the low-speed, high angle of attack characteristics of a complete 4-engine transport aircraft configuration consisting of fuselage, sponson, and wing with high-lift system including flap track fairings as well as the wing-mounted nacelles and propellers. The mesh generation was performed using the CentaurSoft Centaur mesh generation software [1], which is the primary grid generation tool for unstructured application at DLR. Three grid blocks with overlapping boundaries as required for the

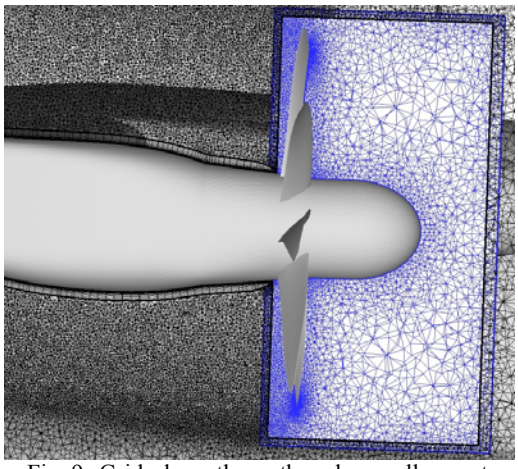

Fig. 9 Grid along the outboard propeller centre-line (propeller-fixed Chimera grid in blue)

Chimera grid approach used here. The first is the hybrid grid about the aircraft, which employs 25 layers of prismatic elements for the resolution of boundary layers and contains refined mesh regions aft of the propellers to properly capture the complex propeller-slipstream wing interaction in the CFD simulation. The other two blocks are for each of the two wing-mounted propellers. Here, tetrahedral meshes are used to reduce the number of grid nodes. The complete three-block Chimera mesh has just over 36 million nodes. Figure 9 shows a cut through the grid along the centreline of the outboard propeller, highlighting the Chimera grid as well as the refinement in the region aft of the propeller for proper slipstream resolution.

Unsteady simulations were run on up to 96 nodes of a large-scale Linux-based cluster making use of dual time stepping, central discretization with matrix dissipation and the Spalart-Allmaras turbulence model as modified by Edwards. The aim of the study was the detailed analysis and study of the complex interactions of the propeller slipstream with the aircraft components as well as the validation of the results using a comprehensive set of data gained from previous wind tunnel tests. Figure 10 shows a comparison between wind tunnel data in the form of a pressure sensitive paint (PSP) measurement on the wing suction side between the propellers and the TAU results time-averaged over one full propeller rotation. The figure indicates a generally quite good agreement of the global flow topology, which clearly shows the propeller slipstream effect on the leading edge suction peaks on the wing and on the high-lift system. Deviations, generally a slight over-prediction in suction peak magnitudes particularly for the high-lift system, can be attributed to the inviscid modelling of the propeller. This approach causes the propeller slipstream to have higher velocities as the blade wake deficit is not accounted for. Figure 11 shows the complex vortex system as simulated for the outboard wing region, which includes both wing tip and flap edge vortices. The refined mesh regions mentioned above allowed to capture and to sustain the propeller tip vortices and blade wakes very nicely as they interact with the wing and high-lift system.

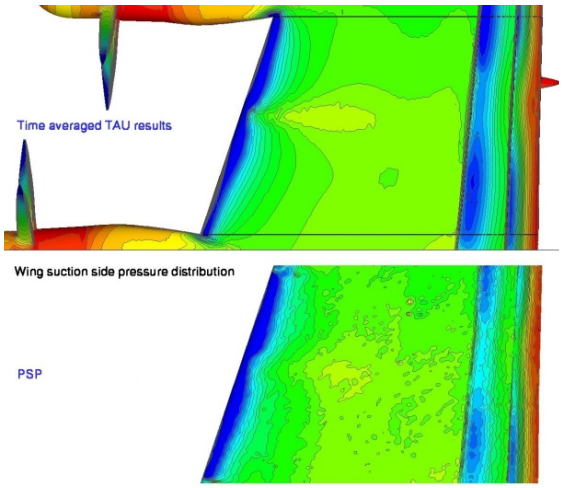

Fig. 10 Comparison of PSP experimental and time averaged CFD data on wing suction side

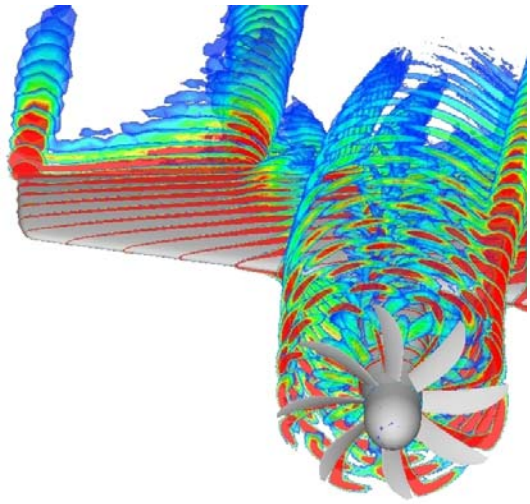

Fig. 11 CFD results of the complex vortex system and propeller-airframe interaction effects

The detailed analysis of the unsteady TAU results in combination with the wind tunnel data has allowed for a much improved understanding of the complicated low-speed aerodynamics of propeller-airframe interactions for complex modern military transport aircraft configurations. The quality of the achieved results underlines the applicability and flexibility of the DLR TAU-Code to the CFD simulation of complex configurations.

Analysis of a delta wing fighter configuration by Delayed DES

While the flow physics of generic delta wings with sharp leading edges are largely understood, realistic configurations with rounded leading edges and canards are still of scientific and industrial interest. The goals of this work is the investigation of a realistic delta wing configuration at 15° angle of attack (see Fig. 12) and at high Reynolds number in comparison with detailed wind tunnel measurements. Former studies have shown the superior results of large and Detached-eddy simulations for delta wings in comparison with RANS computations. As the original DES formulation [11] of has shown the drawback

of only grid based prediction of the boundary layer edge the technique of Delayed DES (DDES) [12] was developed some years ago. This approach is based on a simple modification of the original formulation to provide a dependency of the RANS-LES switch on turbulent flow properties. Results from simulations employing DES and DDES are compared with data from the TU Munich wind tunnel facility to investigate the improvements in DDES. Comparisons of statistical data as well as velocity spectra in the flow field with experiments are performed indicating improvement through DDES, as shown for example in Fig. 13 for RMS distributions.

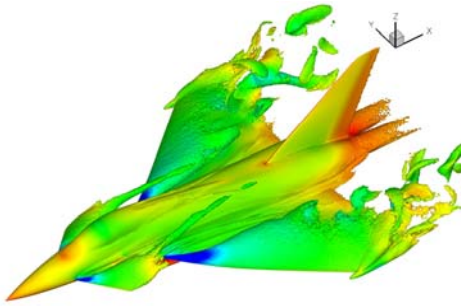

Fig. 12 DDES of the FA5 Configuration at M=0.125, Re=2.7 10^6, α=15°. Iso-vorticity coloured by pressure coefficient.

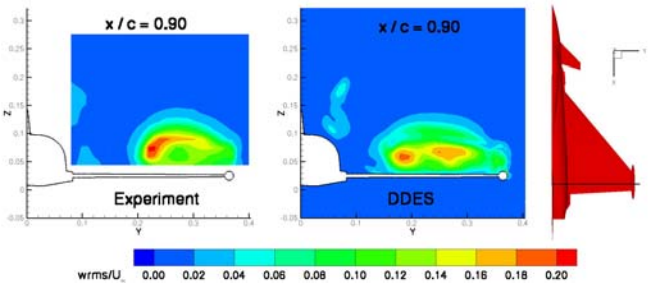

Fig. 13 RMS values of the velocity component normal to the wall. Left: experiment, right: DDES Simulation.

Multidisciplinary simulation of the Ariane-5 nozzle section using DES

For future rocket technologies a deeper insight into the unsteady phenomena during the start phase of modern launchers is essential. Especially unsteady interactions and resonances of flow separation inside the nozzle, the turbulent launcher wake and the nozzle structure will play an important role for the design of future main stage propulsion systems. This so called buffeting coupling phenomenon is one of the main challenges during ascent. In the present study of the Ariane-5 launcher a coupled simulation of the after body with a realistic structural and aerodynamic representation of the Vulcain-2 nozzle is carried out. DES results are coupled with structural computations of the nozzle section. The resulting structural as well as aerodynamic resonances and loads on the nozzle are evaluated. A typical Mach number field for

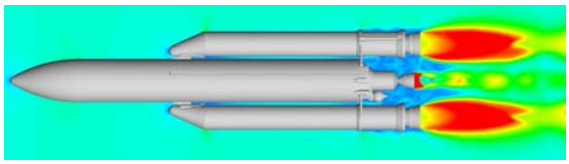

Fig. 14 Mach number contours of the Ariane-5 launcher at M_∞ = 0.8. Steady RANS simulation.

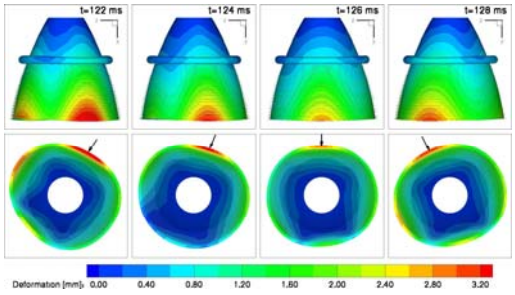

Fig. 15 Deformation of EPC nozzle at four different times, 30 times exaggerated view.

the configuration, including nozzle flow and plume is shown in Fig. 14. A wide spectrum of natural oscillations could be investigated on the nozzle. The shapes and the surface deformations, resulting from the coupled simulations over a period of 6ms are shown in Fig. 15, seen from side and bottom. As visible, mainly an ovalization mode of the nozzle is superimposed by other modes, resulting in a rotation of the minima and maxima of the deformation. The position of the minimum in the nozzle radius is marked in the lower figures by arrows. The counter clockwise rotation of this position is obvious.

4. CONCLUSIONS

A concise overview on the TAU system for flow simulation on unstructured grids and its capabilities has been given. The sample applications presented were chosen to indicate at least partly the spectrum of its

use in solving complex aerodynamic problems with encouraging and often very good results, although the space limitation did not allow a full appreciation of all TAU features, leaving out also applications performed in the aerospace industry.

Despite the high level of numerical flow simulation established today there is still a demand for more accuracy and especially for faster response times. In addition to further improvements to satisfy this demand even for problems of high complexity, it is necessary to extend the system capabilities to user-friendly multidisciplinary optimisation as well as to more complex multi-disciplinary simulations. Work in these directions is under ways in the newly founded *Center for Computer Applications in AeroSpace Science and Engineering* ($C^2A^2S^2E$) and other national projects.

ACKNOWLEDGEMENT

The authors we would like to acknowledge the support which the development of TAU has received over the time from numerous European and national project (like FLOMANIA, DESider, EUROLIFT, MEGADESIGN,…) and DLR projects which are too numerous to be all mentioned by name.

REFERENCES

[1] CentaurSoft. http://www.centaursoft.com. web page, 2007.

[2] Dietz, G., Schewe, G., Kießling, F., Sinapius, M., "Limit-Cycle-Oscillation Experiments at a Transport Aircraft Wing Model", Proceedings of the International Forum on Aeroelasticity and Structural Dynamics IFASD 2003, Amsterdam, The Netherlands, 2003.

[3] Dietz, G., Schewe, G., Mai, H.: "Experiments on heave/pitch limit cycle oscillations of a supercritical airfoil close to the transonic dip", Journal of Fluids and Structures, V19, pp1-16, 2004.

[4] Eliasson, P., "Numerical validation of half model high-lift configuration in a wind tunnel", *45th AIAA Aerospace Science Meeting and Exhibit*, AIAA-2007-262, Reno, Nevada, USA, January 2007.

[5] Frhr. von Geyr, H.; et.al "CFD Prediction of the Maximum Lift Effects on Realistic High Lift Commercial Aircraft Configurations within the European project EUROLIFT II" , *25th AIAA Applied Aerodynamics Conference*, AIAA-2007-4296, Miami, Florida, USA, June 2007.

[6] Puffert-Meißner, W., "The DLR F11 (KH3Y) Model Configurations used in the EUROLIFT Programm, Technical Report IB 124-2004/9, DLR, Braunschweig, Germany, March 2004.

[7] Rudnik, R., "Description of Test Case 214", EUROLIFT, Technical Note EL-TN-2.1.2-1, DLR, Braunschweig, Germany, Sep. 2004.

[8] Rudnik, R.:"The European High Lift Project EUROLIFT II – Objectives, Approach and Structures", *25th AIAA Applied Aerodynamics Conference*, AIAA-2007-4296, Miami, Florida, USA, June 2007.

[9] Schwamborn, D., Gerhold, Th. and Heinrich, R., "The DLR TAU-Code: Recent Applications in Research and Industry", Invited lecture, Proceedings of ECCOMAS CDF 2006, Netherlands, 04.-08.09.2006

[10] Smith, A.M.O. "High-Lift Aerodynamics", 37th Wright Brothers Lecture, AIAA Paper No. 74-939, AIAA 6th Aircraft Design, Flight Test and Operations Meeting, Los Angeles, CA, August 12-14, 1974.

[11] Spalart, P.R., Jou, W.-H., Strelets, M., Allmaras, S.R., 1997: Comments on the feasibility of LES for wings and on a hybrid, RANS/LES approach. In Liu, C. and Liu, Z. (eds) Advances in DNS/LES, *Proceedings of 1st AFOSR International Conf. on DNS/LES,* Ruston, LA, August, 4-8, Greyden Press, Columbus, OH, 1997, pp. 137-147.

[12] Spalart, P.R., Deck, S., Shur, M.L., Squires, K.D., Strelets, M.Kh., and Travin, A., 2006: A New Version of Detached-eddy Simulation, Resistant to Ambiguous Grid Densities, Theoretical and Computational Fluid Dynamics, v. 20, No.3, pp.181-195.

[13] Stürmer, A.: "CFD Validation of Unsteady Installed Propeller Flows using the DLR TAU-Code"; CEAS-2007-104; 1st European Air and Space Conference; Berlin, Germany; 2007.

[14] van den Berg, B., "Boundary Layer Measurements on a Two-Dimensional Wing with Flap", National Aerospace Laboratory – NLR, Amsterdam, The Netherlands, NLR TR 79009 U, January 1979.